

OPTICAL TRAPPING OF CARBON NANOTUBES AND GRAPHENE

S. VASI,^{a,b} M. A. MONACA,^{a,b} M. G. DONATO,^a F. BONACCORSO,^c G. PRIVITERA,^c
O. TRUSHKEVYCH,^c G. CALOGERO,^a B. FAZIO,^a A. IRRERA,^a M. A. IATÍ,^a
R. SAIJA,^b P. DENTI,^b F. BORGHESE,^b P. H. JONES,^d A. C. FERRARI,^c
P. G. GUCCIARDI,^a AND O. M. MARAGÓ^{a,*}

ABSTRACT. We study optical trapping of nanotubes and graphene. We extract the distribution of both centre-of-mass and angular fluctuations from three-dimensional tracking of these optically trapped carbon nanostructures. The optical force and torque constants are measured from auto and cross-correlation of the tracking signals. We demonstrate that nanotubes enable nanometer spatial, and femto-Newton force resolution in photonic force microscopy by accurately measuring the radiation pressure in a double frequency optical tweezers. Finally, we integrate optical trapping with Raman and photoluminescence spectroscopy demonstrating the use of a Raman and photoluminescence tweezers by investigating the spectroscopy of nanotubes and graphene flakes in solution. Experimental results are compared with calculations based on electromagnetic scattering theory.

1. Introduction

Optical trapping of nanostructures has great potential for top-down organization of complex nano-assemblies [1, 2] and increased space and force resolution in photonic force microscopy (PFM) [3, 4]. The small transverse size of carbon nanotubes is the key to achieve nanometric resolution in PFM applications[5], while an axial dimension in the micron range ensures stable trapping and force sensing in the femtonewton regime[3]. Graphene is the prototype 2d material and, as such, has unique mechanical, thermal, electronic, and optical properties, already proven outstanding for both fundamental research and applications[6, 7]. Here we discuss results on optical trapping, force sensing and spectroscopy with nanotubes and graphene.

2. Experimental

Carbon nanotubes dispersions are prepared using purified HiPCO and CoMoCat single wall nanotubes (SWNT) in water with sodium dodecyl benzene sulphonate[3]. Solutions are ultrasonicated and ultracentrifuged before performing optical trapping experiments. Graphite is exfoliated by ultrasonication in a water-surfactant solution (we use dihydroxy sodium deoxycholate (SDC) as surfactant), followed by ultracentrifugation[8]. We do not use any functionalization nor oxidation, in order to retain the electronic structure of pristine graphene in the exfoliated layers[6, 7].

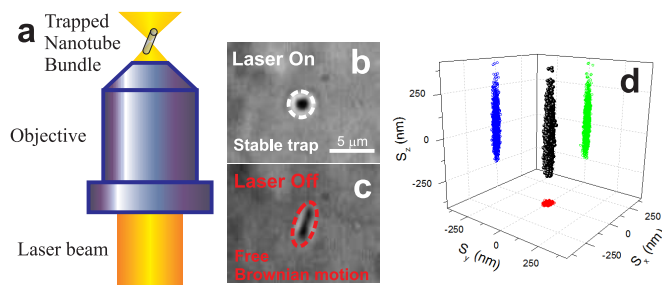


Figure 1. (a) Optical trapping geometry. (b) Image of a trapped nanotube bundle oriented by radiation torque along the optical axis. (c) Image of the same bundle un-trapped (laser is off) and randomly oriented by Brownian motion. (d) Tracking of a trapped nanotube bundle Brownian motion. The calibration of the trap allows force sensing with femtonewton resolution in liquid environment.

Our optical tweezers set-ups[8] have an inverted configuration (*i.e.*, the light propagates upwards) and are equipped with an Olympus Uplan FLN $\times 100$ NA 1.3 objective, which tightly focusses a near infra-red (NIR) and red laser beam for optical trapping, imaging and Raman scattering. The NIR laser tweezers is equipped with a 830nm diode laser (~ 16 mW on the sample). Particle motion is detected by means of back focal plane (BFP) interferometry[5], whereby the interference pattern between forward scattered and unscattered light in the back aperture of the microscope condenser is imaged onto a four-quadrant photodiode (QPD). The outputs from all quadrants are processed as pairwise sums in order to have signals proportional to the trapped particle displacement in the three directions (particle tracking signals). The integration of Raman spectroscopy is obtained using the beam of a He-Ne laser at 633nm[8]. The laser beam is reflected towards the microscope objective focusing on a diffraction limited spot. The backscattered light passes through the edge filter, used for Rayleigh scattering removal, and is subsequently focused by a 50mm lens onto a Jobin-Yvon Triax 190 spectrometer. An avalanche photodiode is used for light detection. Raman spectra are typically acquired with integration times of 0.1-1sec. Setting the monochromator slits to $100\mu\text{m}$ yields a resolution of 10cm^{-1} guaranteeing good S/N ratio even for 100ms integration.

3. Results and Discussion

In our experiments tracking signals are recorded and analyzed by correlation function analysis of fluctuations[3, 9, 10]. For spherical particles correlation functions show a single exponential decay at a relaxation frequency related to trapping force and particle mobility. Instead for nanotubes and graphene we show that the autocorrelations of the transverse detector signals contain combined information on center-of-mass and angular fluctuations and decay with time as a double-exponential with separated positional and angular relaxation frequencies. Furthermore the cross-correlations of the transverse signals decay as single exponentials with relaxation rates related to optical torque and nanotubes and graphene rotational mobility.

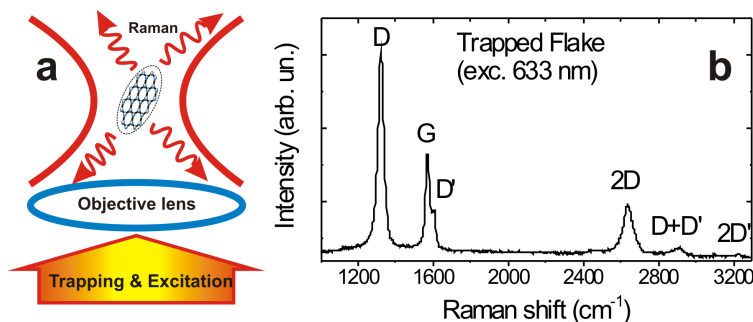


Figure 2. (a) Sketch of the Raman Tweezers setup. Trapping and excitation is performed with the same laser beam at 633nm. Collection of the Raman signal is guided through the same objective used for trapping. (b) Typical Raman spectrum for single layered graphene in the optical trap.

3.1. Force sensing with nanotubes. The combined force and torque measurements enable the full calibration of the optical tweezers when using nanotubes as force sensing probes in the femtonewton regime. Figure 1d shows the Brownian motion of a trapped nanotubes bundle with a size of 10nm and a length of 3 μm as reconstructed through the tracking of the fluctuating signals. Histograms of the transverse fluctuations ensure spatial resolution within 10nm. We estimated the force resolution by accurately measuring the pressure of an additional laser beam at 417nm on a trapped SWNTs bundle in the NIR in a double frequency optical tweezers. For 170 μW of blue light incident on the trapped nanotubes, we measure a shift of $19 \pm 2\text{nm}$ on the optical axis with respect to the equilibrium position without blue light. This corresponds to a radiation pressure of $16 \pm 3\text{fN}$ acting on the trapped nanotubes demonstrating the potential of trapped nanotubes as femtonewton sensors.

3.2. Raman Tweezers on Graphene. We demonstrate optical trapping of individual graphene flakes. This enables the investigation of the anisotropic Brownian particle dynamics in the NIR optical trap, and direct measurement of force and torque constants. Furthermore Raman tweezers provide the unique opportunity to characterize graphene flakes directly in the liquid environment with potential for all-optical sorting.

A typical Raman spectrum of trapped flakes measured at 633nm is plotted in Fig. 2b. Besides the G and 2D peaks, this has significant D and D' intensities, and the combination mode D+D' at 2950 cm^{-1} . The 2D peak is a single band in monolayer graphene, whereas it splits in four in bilayer graphene, reflecting the evolution of the band structure[11]. The large intensity of the D peak in Fig. 2b is assigned to the edges of our sub-micrometer flakes[12]. We note that the 2D band, although broader ($40\text{-}50\text{ cm}^{-1}$) than in pristine graphene[11], is well fitted by a single Lorentzian lineshape, i.e., the flakes are monolayers or they are electronically almost decoupled in the case of few layer graphene.

3.3. Theory. We calculate the radiation force and torque on carbon nanotubes and graphene using the full scattering theory in the framework of the T-matrix approach[13, 14]. We

first consider the incident field configuration in the focal region of a high NA lens in absence of any particle[13]. The radiation force \mathbf{F}_{Rad} and torque \mathbf{G}_{Rad} are calculated considering linear and angular momentum conservation for the combined system of field and particle[14]. In particular, in the case of graphene the dielectric constant is a highly anisotropic tensor[15, 16] with components ε_{\perp} and ε_{\parallel} in the directions perpendicular and parallel to the c axis.[16] For $\lambda=830\text{nm}$, the graphene refractive index is $n_{\perp} = 3+i\,1.5$ and $n_{\parallel} = 1.694$ [16]. We get that stable trapping is achieved when the flake plane is orthogonal to the polarization axis. Instead when the polarization axis lies on the flake plane, the radiation pressure is so strong that the flake is pushed out of the trap. This is a consequence of the large imaginary part of ε_{\perp} . Flat micro-particles with pronounced shape anisotropy, but no optical anisotropy generally orient in an optical trap with their basal plane parallel to the incident polarization axis. In the case of graphene, a significant difference in trapping behavior arises due to the anisotropic optical constants, resulting in an orientation orthogonal to the incident polarization axis. This is related to the strong optical anisotropy of graphene resulting in an orientation dependent radiation pressure. Thus, there is an interplay between optical and shape anisotropy, crucial in determining the diffusion of graphene in the optical trap.

In conclusion, we optically trapped and spectroscopically resolved individual nanotubes bundles and graphene flakes, revealing their angular fluctuations and elucidating their anisotropic dynamics and hydrodynamics. We calculated the radiation force and torque from a full electromagnetic scattering theory showing that orientation in the optical trap is driven by light propagation and polarization. Moreover we integrated Raman spectroscopy with optical trapping allowing for a in liquid spectroscopy of nanotubes and graphene. Our investigation of trapped carbon nanotubes and graphene demonstrates that the optical trap provides an ideal environment for spectroscopic and mechanical probing of such structures.

References

- [1] P.J. Pauzauskie, et al. *Nature Mat.*, **5**, 97 (2006).
- [2] O.M. Maragó, et al. *Physica E*, **40**, 2347 (2008).
- [3] O. M. Maragó, et al. *Nano Lett.*, **8**, 3211 (2008).
- [4] D. Carberry, et al. *Nanotechnology*, **21**, 175501 (2010).
- [5] A. Pralle, et al. *Microscopy Research and Tech.*, **44**, 378 (1999).
- [6] K. S. Novoselov, et al. *Science*, **306**, 666 (2004).
- [7] F. Bonaccorso, et al. *Nat. Photon.*, **4**, 611 (2010).
- [8] O. M. Maragó, et al. *ACS Nano*, **4**, 7515 (2010).
- [9] P. H. Jones, et al., *ACS Nano*, **3**, 3077 (2009).
- [10] G. Volpe, et al., *Phys. Rev. Lett.*, **97** 210603 (2006).
- [11] A. C. Ferrari, et al., *Phys. Rev. Lett.*, **97**, 187401 (2007).
- [12] C. Casiraghi, et al., *Nano Lett.*, **9**, 1433 (2009).
- [13] F. Borghese, et al., *Optics Express*, **15**, 11984 (2007).
- [14] F. Borghese, et al., *Phys. Rev. Lett.*, **100**, 163903 (2008).
- [15] R. R. Nair, et al., *Science*, **320**, 1308 (2008).
- [16] V. G. Kravets, et al. *Phys. Rev. B*, **81**, 155413 (2010).

-
- ^a CNR-IPCF, Istituto per i Processi Chimico-Fisici
Consiglio Nazionale delle Ricerche
I-98158 Messina, Italy
- ^b Università degli Studi di Messina
Dipartimento di Fisica della Materia e Ingegneria Elettronica
I-98166 Messina, Italy
- ^c University of Cambridge
Department of Engineering
CB3 0FA Cambridge, United Kingdom
- ^d University College London
Department of Physics and Astronomy
WC1E 6BT London, United Kingdom
- * To whom correspondence should be addressed | Email: marago@me.cnr.it

Paper presented at the ELS XIII Conference (Taormina, Italy, 2011), held under the APP patronage; published online 15 September 2011.

© 2011 by the Author(s); licensee *Accademia Peloritana dei Pericolanti*, Messina, Italy. This article is an open access article, licensed under a [Creative Commons Attribution 3.0 Unported License](#).